Chin. J. Astron. Astrophys. Vol. 1, No. 1, (2001) 77–84

Chinese Journal of Astronomy and Astrophysics

Coronal Magnetic Flux Rope Equilibria and Magnetic Helicity

You-Qiu Hu⋆, Yan-Wei Jiang and Wei Liu

Department of Earth and Space Science, University of Science and Technology of China, Hefei 230026

Received 2000 October 30; accepted 2000 December 28

Abstract Using a 2.5-dimensional (2.5-D) ideal MHD model, this paper analyzes the equilibrium properties of coronal magnetic flux ropes in a bipolar ambient magnetic field. It is found that the geometrical features of the magnetic flux rope, including the height of the rope axis, the half-width of the rope, and the length of the vertical current sheet below the rope, are determined by a single magnetic parameter, the magnetic helicity, which is the sum of the self-helicity of the rope and the mutual helicity between the rope field and the ambient magnetic field. All the geometrical parameters increase monotonically with increasing magnetic helicity. The implication of this result in solar active phenomena is briefly discussed.

Key words: Sun: magnetic fields – Sun: magnetic flux rope – Sun: magnetic helicity

1 INTRODUCTION

Observations show that the magnetic helicity of solar magnetic structures has a predominant sign in each hemisphere of the Sun, positive in the southern hemisphere and negative in the northern, regardless of the solar cycle (Rust, 1994). The magnetic helicity is strictly conserved in the frame of ideal MHD (Woltjer, 1958), and approximately conserved in the presence of resistive dissipation and magnetic reconnection in a highly conductive plasma (Taylor, 1974; Berger, 1984; Hu et al., 1997). Therefore, during the ceaseless evolution of active regions the magnetic helicity will be continuously accumulated in the corona, and then escapes from the corona by prominence eruptions or coronal mass ejections into interplanetary space in the form of magnetic clouds (Low, 1993). The magnetic flux rope is a typical magnetic structure in the corona, and coexists generally with a prominence of reverse magnetic topology, serving as a habitat of magnetic helicity (Low & Hundhausen, 1995). An extensive study was carried out on the equilibrium properties and catastrophic behavior of coronal magnetic flux ropes (Van Tend & Kuperus, 1978; Forbes & Isenberg, 1991; Isenberg et al., 1993; Lin et al., 1998), and useful explorations proceeded with the possibility for the ropes to induce solar flares (Forbes, 1991;

⋆ E-mail: huyq@ustc.edu.cn

Forbes & Priest, 1995) and coronal mass ejections (Forbes, 1990; Forbes & Isenberg, 1991; Guo et al., 1996; Wu & Guo, 1999). Previous investigations of magnetic flux ropes were limited to line current (Van Tend & Kuperus, 1978) or thin-rope (Forbes & Isenberg, 1991; Isenberg et al., 1993; Lin et al., 1998) approximations, using either the axial current intensity or the magnetic energy to characterize the physical properties of the ropes. However, a realistic magnetic flux rope has a transverse width close to the height of its axis, while the axial current intensity and the magnetic energy of the rope are not conserved during the evolution of the rope. Recently, Hu & Liu (2000, referred to as Paper I hereinafter) presented a numerical study of large-radius coronal magnetic flux ropes, in which conserved quantities, such as the axial and annular magnetic fluxes and the magnetic helicity, were adopted to describe the physical properties of the ropes, and relationships were established between the geometrical parameters, including the height of the rope axis, the half-width of the rope, and the length of the vertical current sheet below the rope, and the conserved magnetic parameters mentioned above. Their results showed that the geometrical parameters increase monotonically and smoothly with increasing magnetic parameters, and no catastrophe occurs. In Paper I, the ambient magnetic field is a bipolar closed field, the magnetic flux rope emerges from the photosphere, and all the conserved quantities of the rope are controlled by a single emergence parameter, so that they cannot be adjusted independently. Consequently, that paper failed to answer the question which of the three conserved quantities determines the equilibrium properties of the rope, and failed to establish a definite relation between the geometrical parameters and the magnetic helicity. This paper starts with a coronal flux rope in equilibrium embedded in the bipolar ambient magnetic field; at time $t = 0$, the axial and annular magnetic fluxes of the rope are abruptly changed, and then the system is let to evolve to a new equilibrium. The relation between the geometrical parameters and the magnetic helicity for the equilibrium is then established on this basis.

2 MAGNETIC HELICITY OF CORONAL MAGNETIC ROPES

Take a Cartesian coordinate system such that the photosphere coincides with the x-z plane and the y-axis is vertical and upward. For a two-dimensional problem independent of z, one may introduce a magnetic flux function $\psi(t, x, y)$ related to the magnetic field by

$$\boldsymbol{B} = \nabla \times (\psi \hat{\mathrm{z}}) + B_z \hat{\boldsymbol{z}} \,. \tag{1}$$

Following Hu et al. (1997), the two-dimensional magnetic helicity in a volume V reads

$$H_T = \int_V \psi B_z \, \mathrm{d}V \,. \tag{2}$$

This magnetic helicity is related to the conventional magnetic helicity

$$H = \int_V \boldsymbol{A} \cdot \boldsymbol{B} \, \mathrm{d}V \,, \tag{3}$$

($\boldsymbol{A}$ is the vector potential) by

$$H = 2H_T + \oint_\sigma (\boldsymbol{A}_z \times \boldsymbol{A}_p) \cdot \mathrm{d}\boldsymbol{S} \,, \tag{4}$$

where σ is the boundary of V, $\boldsymbol{A}_z$ and $\boldsymbol{A}_p$ satisfy

$$\boldsymbol{A} = \boldsymbol{A}_z + \boldsymbol{A}_p \,, \quad \nabla \times \boldsymbol{A}_p = B_z \hat{\boldsymbol{z}} \,, \quad \boldsymbol{A}_z = \psi \hat{\boldsymbol{z}} \,. \tag{5}$$

Let us now determine the magnetic helicity of the coronal rope in terms of Equation (4). For a segment of the rope of unit length along the z-direction, σ consists of the side face, the bottom, and the top. The problem being two-dimensional, only the side face makes a contribution to the surface integral on the right hand side of Equation (4). Moreover, $\psi = \text{const}$ along the side face, set to be Φ_c, which represents the annular magnetic flux of the ambient magnetic field outside of the rope per unit length along the z-direction, if ψ is set to be zero at infinity. In this situation,

$$\oint_\sigma (\boldsymbol{A}_z \times \boldsymbol{A}_p) \cdot \mathrm{d}\boldsymbol{S} = \oint_\sigma \Phi_c(\hat{\boldsymbol{z}} \times \boldsymbol{A}_p) \cdot \mathrm{d}\boldsymbol{S} = -\int_V \Phi_c \hat{\boldsymbol{z}} \cdot \nabla \times \boldsymbol{A}_p \mathrm{d}V = -\Phi_c \Phi_z \,, \tag{6}$$

where

$$\Phi_z = \int_{\psi \geq \Phi_c} B_z \mathrm{d}x\mathrm{d}y \tag{7}$$

is the axial magnetic flux of the rope. The annular magnetic flux of the rope over a unit length along the z-direction is the difference between the magnetic flux function at the rope axis and Φ_c, denoted as Φ_p. Inserting Equation (6) into (4) leads to the following expression for the magnetic helicity of the rope of unit length:

$$H = 2H_T - \Phi_c \Phi_z \,, \tag{8}$$

where

$$H_T = \int_{\psi \geq \Phi_c} \psi B_z \mathrm{d}x\mathrm{d}y \,. \tag{9}$$

Define

$$H_{T0} = \int_{\psi \geq \Phi_c} (\psi - \Phi_c) B_z \mathrm{d}x\mathrm{d}y = H_T - \Phi_c \Phi_z \,, \tag{10}$$

which is entirely determined by the magnetic structure inside the rope and has nothing to do with the ambient magnetic field. As a matter of fact, H_{T0} stands for one half of the self-helicity of the rope. An increase of ψ and B_z inside the rope results in a corresponding increase in the annular and axial magnetic fluxes respectively, accompanied by an increase of the magnetic helicity of the rope. From Equation (10), we may rewrite Equation (8) as follows:

$$H = 2H_{T0} + \Phi_c \Phi_z \,. \tag{11}$$

The first term on the right hand side of Equation (11) is the self-helicity of the rope, and the second stands for the mutual helicity between the rope and the ambient magnetic field. This equation shows that the magnetic helicity depends not only on the axial and annular magnetic fluxes of the rope, but also on the annular magnetic flux of the ambient magnetic field. Note that Φ_c, Φ_z, H_T and H_{T0} are all conserved quantities (see Paper I), so H_T is also conserved. Considering that the computational domain is always finite, part of the annular magnetic flux of the ambient magnetic field must be missing from the domain. As a result, the effective mutual helicity is reduced, and so is H. Therefore, we replace Equation (11) by

$$H_\alpha = 2H_{T0} + \alpha \Phi_c \Phi_z \,, \tag{12}$$

where H_α is called modified magnetic helicity, and α is a constant between 0 and 1. For $\alpha = 1$, Equation (11) is recovered, and the corresponding magnetic helicity will be denoted by H_1 hereinafter.

3 GEOMETRICAL PARAMETERS VERSUS MAGNETIC HELICITY FOR THE ROPE

We use a time-dependent, 2.5-D ideal MHD model to obtain new equilibrium solutions associated with the rope. The basic equations are cast in the non-dimensional form:

$$\frac{\partial \rho}{\partial t} + v_x \frac{\partial \rho}{\partial x} + v_y \frac{\partial \rho}{\partial y} + \rho \frac{\partial v_x}{\partial x} + \rho \frac{\partial v_y}{\partial y} = 0\,, \tag{13}$$

$$\frac{\partial v_x}{\partial t} + v_x \frac{\partial v_x}{\partial x} + v_y \frac{\partial v_x}{\partial y} + \frac{\partial T}{\partial x} + \frac{T}{\rho}\frac{\partial \rho}{\partial x} + \frac{2}{\rho\beta_0}\frac{\partial \psi}{\partial x}\Delta\psi + \frac{2B_z}{\rho\beta_0}\frac{\partial B_z}{\partial x} = 0\,, \tag{14}$$

$$\frac{\partial v_y}{\partial t} + v_x \frac{\partial v_y}{\partial x} + v_y \frac{\partial v_y}{\partial y} + \frac{\partial T}{\partial y} + \frac{T}{\rho}\frac{\partial \rho}{\partial y} + \frac{2}{\rho\beta_0}\frac{\partial \psi}{\partial y}\Delta\psi + \frac{2B_z}{\rho\beta_0}\frac{\partial B_z}{\partial y} + g = 0\,, \tag{15}$$

$$\frac{\partial v_z}{\partial t} + v_x \frac{\partial v_z}{\partial x} + v_y \frac{\partial v_z}{\partial y} + \frac{2}{\rho\beta_0}\frac{\partial \psi}{\partial x}\frac{\partial B_z}{\partial y} - \frac{2}{\rho\beta_0}\frac{\partial \psi}{\partial y}\frac{\partial B_z}{\partial x} = 0\,, \tag{16}$$

$$\frac{\partial \psi}{\partial t} + v_x \frac{\partial \psi}{\partial x} + v_y \frac{\partial \psi}{\partial y} = 0\,, \tag{17}$$

$$\frac{\partial B_z}{\partial t} + v_x \frac{\partial B_z}{\partial x} + v_y \frac{\partial B_z}{\partial y} + B_z \frac{\partial v_x}{\partial x} + B_z \frac{\partial v_y}{\partial y} - \frac{\partial v_z}{\partial x}\frac{\partial \psi}{\partial y} + \frac{\partial v_z}{\partial y}\frac{\partial \psi}{\partial x} = 0\,, \tag{18}$$

$$\frac{\partial T}{\partial t} + v_x \frac{\partial T}{\partial x} + v_y \frac{\partial T}{\partial y} + (\gamma - 1)T\frac{\partial v_x}{\partial x} + (\gamma - 1)T\frac{\partial v_y}{\partial y} = 0\,. \tag{19}$$

The notations are conventional and the same as in Paper I. The computational domain is taken to be $0 \le x \le 5$, $0 \le y \le 12$, and discretized into a 50×60 uniform mesh (52×62 grid points). The relevant boundary conditions are the same as those taken in Paper I. We point out in passing that the boundary conditions on the right hand side ($x = 5$) and the top ($y = 12$) are very crucial in finding the equilibrium solutions of ropes with a vertical current sheet of finite length. The inability of a previous paper by Hu & Liu (1999) to produce these solutions is entirely due to the inappropriate boundary conditions at these two boundaries (cf. Hu & Liu, 1999; Hu et al., 2000). The initial state is a solution of Paper I with the emergence parameter $C_E = 8.6$, characterized by a magnetic flux rope attached to the photosphere and surrounded by a bipolar ambient magnetic field. Figure 1a shows the magnetic configuration for the initial state. The height of the rope axis is $h_a = 1.82$, the half-width of the rope is $w = 1.34$, and the length of the vertical current sheet is $h_s = 0$. The conserved quantities of the rope are $\Phi_z = 21.1$, $H_{T0} = 44.7$, and $\Phi_p = 3.02$ whereas the total annular magnetic flux of the ambient magnetic field is $\Phi_c = 3\pi = 9.42$. Starting from this initial state, we change the magnetic flux function $\psi_0(x, y)$ and the axial magnetic field $B_{z0}(x, y)$ inside the rope ($\psi \le \Phi_c$) to

$$\psi(x, y) = \Phi_c + \alpha_\psi[\,\psi_0(x, y) - \Phi_c\,]\,, \quad B_z(x, y) = \alpha_z B_{z0}(x, y)\,, \tag{20}$$

where α_ψ and α_z are positive constants, and then let the system evolve into a new equilibrium. After such a change, the axial and annular magnetic fluxes, Φ_z and Φ_p, increase by a factor of α_ψ and α_z respectively, and the half-self-helicity of the rope, H_{T0}, becomes $\alpha_\psi\alpha_z$ times the initial value accordingly. Figure 1 shows the magnetic configurations at a set of times for the case of $\alpha_\psi = 1.5$ and $\alpha_z = 1$. Owing to the increase of the annular magnetic flux, the magnetic rope expands and ascends, becoming separated from the photosphere and leaving a vertical

current sheet below. After a period of nearly 60 τ_A (τ_A is the Alfvén transit time, see Paper I), the magnetic rope reaches equilibrium. For each set of (α_ψ, α_z) values, an equilibrium state is obtained thorough numerical simulation, along with the geometrical and magnetic parameters of the associated magnetic flux rope. On this basis, a quantitative analysis is made on the relation between the two sets of parameters, especially between the geometrical parameters and the magnetic helicity. Figure 2a shows the geometrical parameters as a function of α_ψ for $\alpha_z = 1$, the case where the axial magnetic flux of the rope is kept constant. All the geometrical parameters increase monotonically with increase of α_ψ or the annular magnetic flux of the rope.

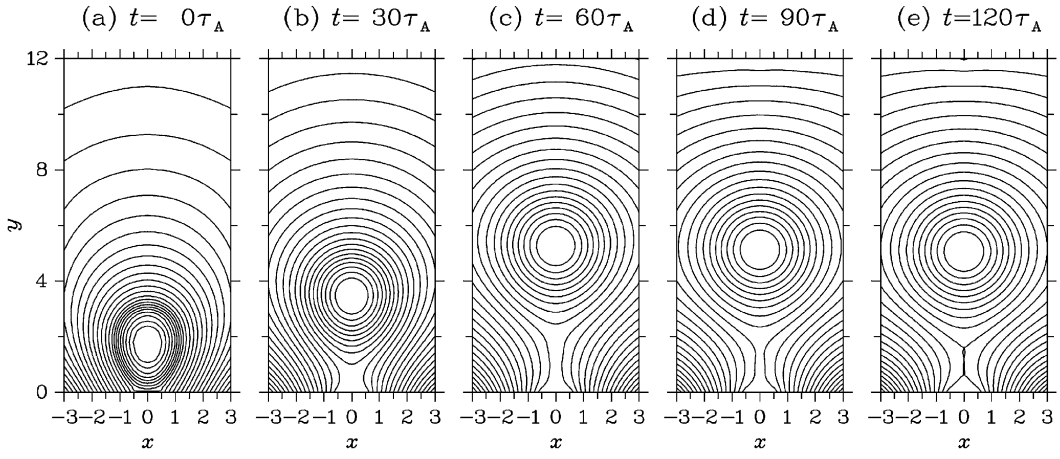

Fig. 1 Magnetic configurations at several separate times for $\alpha_\psi = 1.5$ and $\alpha_z = 1$

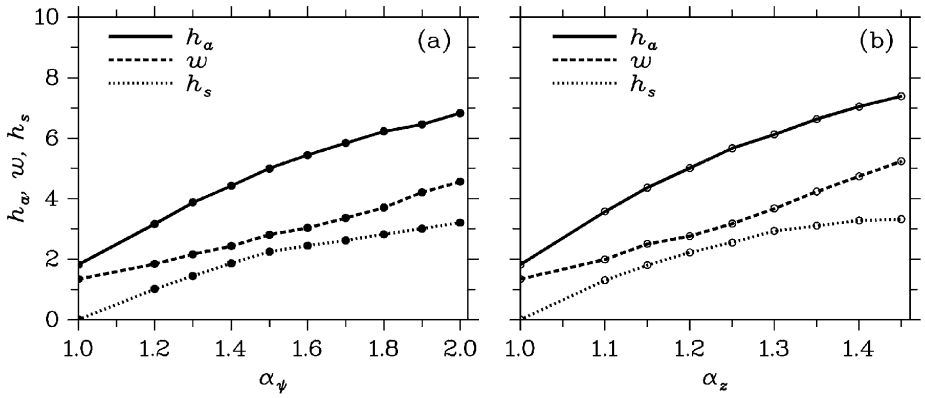

Fig. 2 Geometrical parameters of the magnetic rope versus (a) α_ψ for $\alpha_z = 1$ and (b) α_z for $\alpha_\psi = 1$

Figure 2b shows the geometrical parameters as a function of α_z for $\alpha_\psi = 1$, the case where the annular magnetic flux of the rope is kept constant. The profiles are similar to those in Figure 2a except that the growth amplitude of the geometrical parameters is larger in Figure 2b for the same enhancement factor of magnetic flux, implying that the axial magnetic flux exerts a larger influence on the geometrical parameters of the rope than the annular magnetic flux does. The three panels in Figure 3 represent the geometrical parameters of the rope as

functions of the half-self-helicity H_{T0} (Fig. 3a), of the total magnetic helicity H_1 (Fig. 3b) and of the modified magnetic helicity H_α ($\alpha = 0.7$) (Fig. 3c). There are two curves for each geometrical parameter: the filled circles denote samples for a fixed axial magnetic flux and a variable annular magnetic flux, and the open circles, samples for a fixed annular magnetic flux and a variable axial magnetic flux. The pairs of curves are not coincident in Figs. 3a and 3b, implying that the relation of these parameters to both H_{T0} and H_1 are not single valued. In other words, the geometrical parameters of the rope cannot be uniquely determined by the magnetic parameter H_{T0} or H_1. Comparing Figs. 3a and 3b, it can be seen that the deviation between the two curves of each pair is smaller in Fig. 3b than in Fig. 3a, and this indicates that it is reasonable to include the mutual helicity in the total magnetic helicity of the rope. By contrast, the two profiles of each geometrical parameter as function of the modified magnetic helicity H_α with $\alpha = 0.7$ essentially coincide with each other (Fig. 3c). Therefore, the conclusion mentioned above that the axial magnetic flux has a larger effect on the geometrical parameters is attributed to the fact that an increase of the axial magnetic flux will enhance both the self-helicity and the mutual helicity, whereas an increase of the annular magnetic flux has no bearing on the mutual helicity. Therefore, for the same enhancement factor, an increase of the axial magnetic flux leads to a larger growth of H_α ($\alpha > 0$), and hence a larger increment of the geometrical parameters of the rope. Incidentally, to our knowledge we are the first to simultaneously investigate the roles taken by the axial and annular magnetic fluxes in the behavior of the coronal magnetic flux rope and to make a comparison between them. Previous authors also studied the effect of either the axial magnetic flux (Guo & Wu, 1998) or the annular magnetic flux (Wu et el., 1995; Chen, 1996) on the behavior of the rope, but did not make any comparison between the two cases. Nevertheless, it is quite interesting that a common conclusion was reached by these authors that an injection of either of the axial and annular magnetic fluxes into the rope while keeping the other fixed may drive the eruption of the rope, and this conclusion is essentially consistent with that reached in this study.

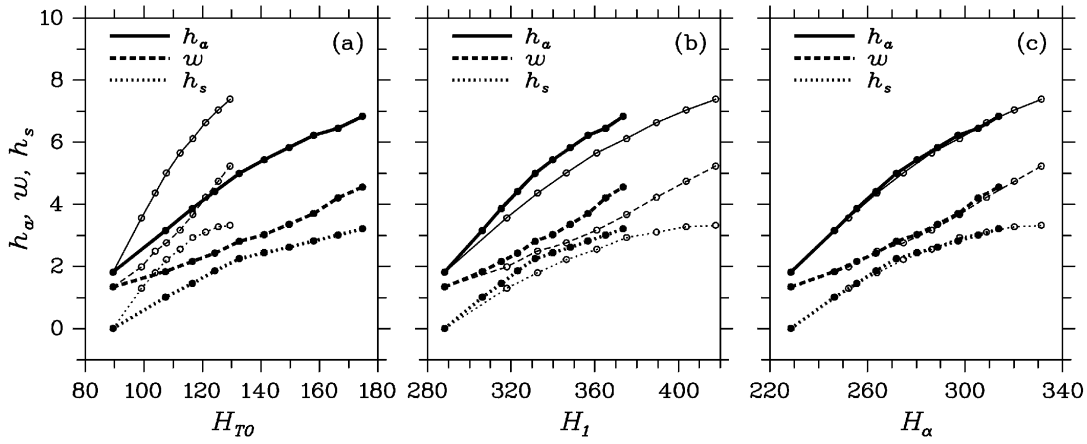

Fig. 3 Geometrical parameters of the magnetic rope versus (a) the half-selfe-helicity H_{T0}, (b) the total magnetic helicity H_1, and (c) the modified magnetic helicity H_α with $\alpha = 0.7$

The modification factor α in Equation (12) is chosen so as to achieve an approximate coincidence between the two sets of profiles. As mentioned above, this is due to the finiteness of the computational domain which reduces the effective mutual helicity. We repeated the

calculations for a larger domain: $0 \leq x \leq 7$, $0 \leq y \leq 24$ (70×120 uniform meshes), and found that $\alpha = 0.96$. The results are shown in Figure 4. We argue that α should approach unity if the domain is further expanded, and conclude that the geometrical parameters of the rope are indeed determined by a single magnetic parameter, namely, the magnetic helicity of the rope, which is the sum of the self-helicity of the rope and the mutual helicity between the rope and the ambient field. We should point out in passing that the geometrical parameters are somewhat smaller in Figure 4 than in Figure 3 for the same set of values of the magnetic parameters. This indicates that the size of the computational domain has a subtle influence on the numerical results associated with the rope. The larger the domain is, the more ambient magnetic flux will be included in the domain. The ambient magnetic field plays a role of hindering the expansion and rising of the embedded rope so that the geometrical parameters of the rope become smaller for a larger computational domain. Nevertheless, the single-valued relation between the geometrical parameters and the modified magnetic helicity is still maintained for the larger computational domain, and what is more, the modified magnetic helicity H_α is closer to the total magnetic helicity H_1 as expected.

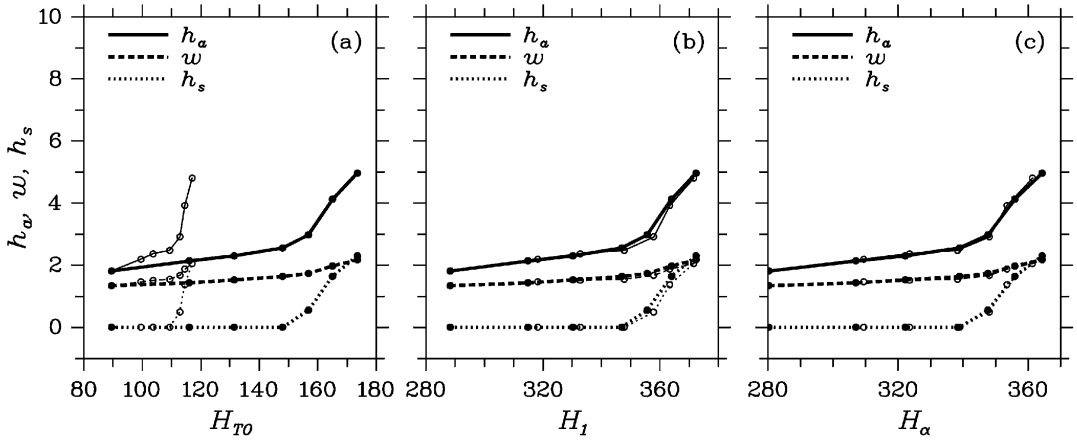

Fig. 4 Same as Fig. 3 but for a larger computational domain ($0 \leq x \leq 7$, $0 \leq y \leq 24$) and $\alpha = 0.96$

4 CONCLUDING REMARKS

Using a 2.5-D ideal MHD model, a numerical study is presented on the equilibrium properties of coronal magnetic flux ropes with emphasis on the dependence of the geometrical parameters on the magnetic parameters. The geometrical parameters of the rope increase monotonically with increasing axial and annular magnetic fluxes and magnetic helicity. The magnetic helicity is the sum of the self-helicity of the rope and the mutual helicity between the rope and the ambient magnetic field. It is shown that a single-valued relationship can be achieved between the geometrical parameters and a modified magnetic helicity, obtained from the total magnetic helicity by a suitable reduction of the share of mutual helicity. The extent to which the share of the mutual helicity is reduced is controlled by a modification factor α (see Equation (12)) that depends on the size of the computational domain. The value of α approaches unity for a sufficiently large domain, as demonstrated by the numerical results. Consequently, we argue that the geometrical parameters of the rope is uniquely determined by

a single magnetic parameter, i.e. the magnetic helicity. This conclusion has certain implications in solar active phenomena. Low (1993) argued that the ceaseless accumulation of magnetic helicity in the corona needs a mechanism by which the accumulated magnetic helicity is removed from the corona, and prominence eruptions and coronal mass ejections are probable candidates. Based on the conclusion that the geometrical conditions of a coronal magnetic flux rope are determined by its magnetic helicity, it may be conjectured that the eruption of the rope will be closely related to its magnetic helicity, too. If this conclusion is correct, one then finds a more natural way to associate the magnetic helicity with relevant solar active phenomena. The present simple model is limited to a specific ambient magnetic field, and the magnetic rope has no catastrophic behavior. It would be undoubtedly interesting to extend the present analysis to other ambient magnetic fields and to catastrophic cases; we relegate this task to future efforts.

Acknowledgements Major Project 19791090 supported by National Natural Science Foundation of China and 973 Project (G2000078404).

References

Berger M. A., 1984, Geophys. Astrophys. Fluid Dyn., 30, 79
Chen J., 1996, J. Geophys. Res., 101, 27499
Forbes T. G., 1990, J. Geophys. Res., 95, 11919
Forbes T. G., 1991, Geophys. Astrophys. Fluid Dyn., 62, 15
Forbes T. G., Isenberg P. A., 1991, ApJ, 373, 294
Forbes T. G., Priest E. R., 1995, ApJ, 446, 377
Guo W. P., Wu S. T., 1998, ApJ, 494, 419
Guo W. P., Wu S. T., Tandberg-Hanssen E., 1996, ApJ, 469, 944
Hu Y. Q., Liu W., 2000, ApJ, 540, 1119 (Paper I)
Hu Y. Q., Liu W., 1999, In: C. Fang, J. C. Hénoux, M. D. Ding, eds., Proc. of the First Franco-Chinese Meeting on Solar Physics, Beijing: International Academic Publishers, 1
Hu Y. Q., Xia L. D., Li X., Wang J. X., Ai G. X., 1997, Solar Phys., 170, 283
Isenberg P. A., Forbes T. G., Démoulin P., 1993, ApJ, 417, 368
Lin J, Forbes T. G., Démoulin P., 1998, ApJ, 504, 1006
Low B. C., 1993, Phys. Plasmas, 1, 1684
Low B. C., Hundhausen J. R., 1995, ApJ, 443, 818
Rust J. D., 1994, Geophys. Res. Lett., 21, 241
Taylor J. B., 1974, Phys. Rev. Lett., 33, 1139
Van Tend W., Kuperus M., 1978, Solar Phys., 59, 115
Woltjer L., 1958, Proc. Nat. Acad. Sci. USA, 44, 489
Wu S. T., Guo W. P., 1999, J. Geophys. Res., 104, 14789
Wu S. T., Guo W. P., Wang J. F. 1995, Solar Phys., 157, 325